Plasmonics (2016) 11:1–9
DOI 10.1007/s11468-015-9977-3

Optical Properties and Liquid Sensitivity of Au-SiO_2-Au Nanobelt Structure

Mehrdad Irannejad[1] · **Bo Cui**[1] · **Mustafa Yavuz**[1]

Received: 16 February 2015 / Accepted: 8 May 2015 / Published online: 2 July 2015

Abstract Optical properties of the Au-SiO_2-Au nanobelt structure with quasiperiodicity along x-axis and fixed Au height, width and different spacer (dielectric) heights were numerically investigated for sensing application of liquids with refractive indices close to the water. Although both propagated surface plasmon mode and localized surface plasmon mode were recorded in the single-layer Au and Au-SiO_2-Au nanobelt structure, only the localized surface plasmon mode was recorded in the Au-SiO_2 nanobelt structure. The effects of increasing the dielectric layer (between two Au nanobelts) height on the extinction spectrum were observed as blue shift of whole extinction spectrum. It was found that the localized surface plasmon mode shift was negligible while the propagated surface plasmon mode was significantly shifted towards smaller wavelength. The minimum resonance linewidth was calculated as 42 nm at refractive index of 1.377, which is much smaller than that in the single-layer Au and Au-SiO_2 nanobelt structures.

Keywords Grating structure · Localized surface plasmon · Hybrid plasmonic mode · Nanobelt · Sensor

Introduction

Resonant oscillation of conduction electrons at the interface between metallic and dielectric materials (surface plasmon) with negative and positive permittivity has gained much attention in sensing applications especially in chemical and biosensing applications in last decades [1, 2]. This broad interest is mainly due to the ability of controlling the gaps between nanostructures to create regions with high enhancement of electromagnetic (EM) field at the materials interface [3, 4].

Besides localized surface plasmon (LSPR), the resonant oscillation of electrons can propagate perpendicular to the incident wavevector (k_z), known as propagating surface plasmon (PSP) [5]. In the last decade, many different nanostructures using noble metals such as gold and silver have been studied to manipulate the optical properties at the nanometre scale for novel applications including bio-/chemical sensors [6, 7], plasmonic waveguides [8], laser [9] and drug delivery [10].

Nanostructures with subwavelength rectangular cross-section were shown with a strong plasmonic mode at the visible region and thus could be considered as promising candidates for sensing applications due to their ability to tune the plasmonic resonance modes to match the biological transparency window and coincide with the light source.

Recently, the optical properties of gold nanobelt (nanowire with rectangular cross-section) structures with different cross-sectional aspect ratio ($\mathrm{AR} = \frac{\mathrm{Width}}{\mathrm{Height}}$) and fixed length were studied by L.J.E. Anderson and co-worker [4]. It was found that the plasmonic mode properties such as linewidth in such structure strongly depends on the x-AR, and the resonance wavelength can be tuned over the visible region by changing the x-AR. For example, a nanobelt with low cross-sectional aspect ratio was shown to have plasmonic resonance mode at green wavelength, while those with larger cross-sectional aspect ratio offer plasmonic mode at red wavelength.

In this paper, we numerically study optical properties of the sandwich nanobelt structure consisting of two gold nanobelts

✉ Mehrdad Irannejad
mehrdad.irannejad@uwaterloo.ca

[1] Waterloo Institute for Nanotechnology, University of Waterloo, Waterloo, ON, Canada

with short length of 1 μm which were separated by a thin layer of dielectric nanobelt spacer. The ability of such structures (single-layer Au nanobelt grating and the Au-SiO_2-Au nanobelt grating) in sensing application is also investigated, and the structural bulk sensitivity and its optical properties are compared.

Methodology

The 3D full wavevector finite difference time domain (FDTD) method, which is a powerful technique in solving Maxwell's equations in a complex geometries and dispersive media, was employed to solve the Maxwell's equations discretely using Yee cells [11] and calculate the extinction spectrum of Au-SiO_2-Au nanobelt in a quasiperiodic structure along x-axis.

The permittivity values of high refractive index glass substrate and superstrate (i.e. target material in sensing application), $\varepsilon(\omega)$, were assumed respectively as 6.25 (n=2.5) and n^2, where n is the refractive index of target liquids. The Au nanobelt permittivity was calculated using Lorantz-Drude model [12, 13] by fitting the empirical data of real and imaginary parts of the gold permittivity over a given wavelength region of interest as shown in Fig. 1.

The FDTD method was carried out using the commercial software package (FDTD Solution) from Lumerical Inc. The plane wave source, nanobelt structure, transmission and reflection monitors were co-planar with boundary conditions that made them effectively infinite. The incident light source was placed in the substrate region to reduce the incident light dispersion. Air was considered as filling material between each grating nanobelt structure and superstrate. In this study, we used a plane wave of wavelength in the range of 300 nm to 1 μm with electric field amplitude of 1 V/m, different polarization angle in the range of 0° (TM-mode) to 90° (TE-mode) and different incident angle in the range of 0° to 30°. The sensing liquids of thickness of 250 nm covered the nanobelt structure and filled the space between them as schematically shown in Fig. 2b, c. The periodic boundary condition was used in x direction. While in the y and z directions, the perfect matching layers (PML) were used to absorb the reflected light back to the nanobelt structure. The calculation grid resolution was as small as 3 nm (grid point-to-point distance) in the simulation cell, and combination of grading mesh and conformal mesh methods was used to calculate the electric and magnetic fields at the corner and square regions of the nanobelts (http://docs.lumerical.com/en/ref_sim_obj_mesh_refinement.html). The calculation time was set as 350 fs, and the extinction (1-T) spectra were calculated using an x-y monitor at 250 nm away from the nanobelt surface. The plane wave source was placed 200 nm underneath the structure inside the substrate material as shown in Fig. 2c.

Results and Discussion

Extinction Resonance Spectrum (Normal Incidence, TM-Mode)

The extinction resonance spectra of single-layer Au nanobelt with 20 nm height and 100 nm width (x-AR=5), the Au-SiO_2 and the Au-SiO_2-Au nanobelt structures with a 10 nm thick SiO_2 as spacer layer (x-AR=5) are shown in Fig. 2d. As can be seen from this figure, for single-layer Au nanobelt structure, there are two extinction peaks at 675 and 987 nm and a shoulder at wavelength of 938 nm, whereas for the Au-SiO_2

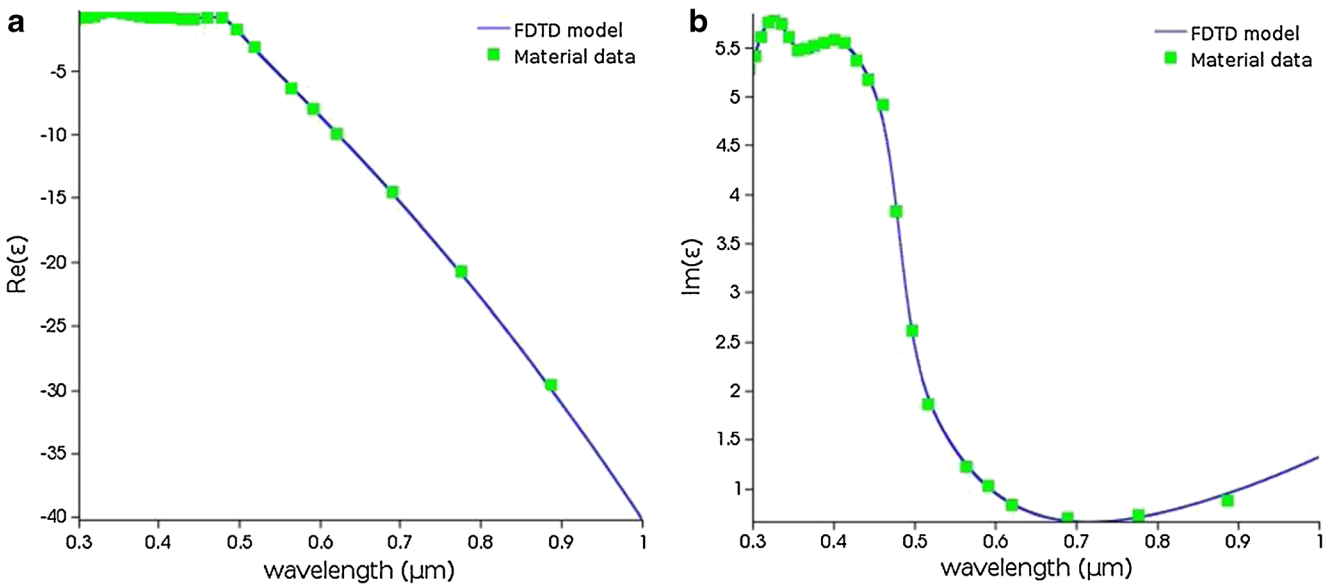

Fig. 1 Real part (**a**) and imaginary part (**b**) of gold permittivity based on Lorantz-Drude mode as a function of wavelength in the range of 300 nm to 1 μm

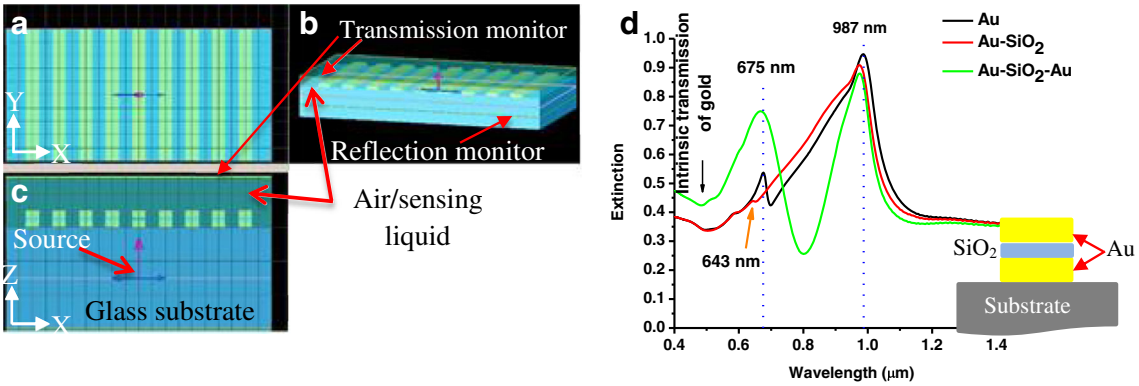

Fig. 2 The FDTD layout of the Au-SiO_2-Au nanobelt in **a** XY view, **b** perspective view and **c** XZ view. **d** FDTD calculated extinction spectrum of quasiperiodic nanobelt structures in single-layer Au, Au-SiO_2 and Au-SiO_2-Au. The Au nanobelt height and width were fixed at 20 and 100 nm, respectively. The structural periodicity along *x*-axis, spacer height and the superstrate refractive index were fixed at 300 nm (centre to centre), 10 nm and 1.0000, respectively

nanobelt structure extinction resonance peak at wavelength of 975 nm was recorded. The propagated surface plasmon resonance (PSPR) along *x* direction at wavelength of 675 nm was in agreement with reported value with *x*-AR=5 and linewidth of 444 nm [4].

From Fig. 2d, it is also clear that by adding 10 nm thick of SiO_2 (Au-SiO_2) the surface plasmon resonance at wavelength of 675 nm was shifted to 643 nm with very low intensity, which could be attributed to phase velocity reduction of the propagating wave [14] as it is also shown in Fig. 3d. Changing the structure to the Au-SiO_2-Au led to strong resonance intensity and a blue shift in the resonance position by 12 and 8 nm, respectively. The resonance peaks of the new structure were recorded at wavelength of 975 and 667 nm. Yet there was no significant change in the position of shoulder peak.

The linewidth of the localized surface plasmon resonance was reduced from 296 to 128 nm as results of adding the spacer and the second Au nanobelt. Furthermore, the linewidth of the propagating surface plasmon resonance mode was increased from 30 to 175 nm compared to the single-layer Au nanobelt structure as can be seen from Fig. 2d and summarized in Table 1. Yet it is smaller than the value reported by Anderson and co-worker [4]. It can also be seen that by adding a spacer nanobelt on top of the Au nanobelt (red curve in Fig. 2d), there was not any variation in the resonance linewidth at wavelength of 975 nm compared to the one in the single-layer Au nanobelt structure at wavelength of 987 nm as it is listed in Table 1.

Figure 3 shows the electric profile of the quasiperiodic single-layer Au nanobelt, the Au-SiO_2 nanobelt and the Au-SiO_2-Au nanobelt structures. Both localized surface plasmon and propagated surface plasmon profile were observed at the Au/glass substrate interface. It was found that by adding a 10 nm thick SiO_2, the resonance peak at wavelength of 675 nm (Fig. 3a) was shifted by 32 nm and appears as resonance peak with very low intensity at wavelength of 643 nm (Fig. 3d) as it was also shown in Fig. 2d. This blue shift results in electric field enhancement reduction at Au/glass substrate interface (Fig. 3d) which is in agreement with the recorded transmission spectrum in Fig. 2d and could be attributed to reduction of phase velocity of the propagating surface plasmon mode (Fig. 4a) (http://docs.lumerical.com/en/ref_sim_obj_mesh_refinement.html).

As it is clear from Figs. 3e and 4b, the resonance mode at wavelength of 938 nm (shoulder peak) was recorded as two localized surface plasmon mode with evanescent tails to the glass substrate and SiO_2 layer, which is similar to the TEM_{10} mode of an optical waveguide with rectangular cross-section [15, 16]. Therefore, electric field enhancement at resonance wavelength of 938 nm was reduced as it is evident by comparing the Fig. 3e, f. Figures 3f and 4c, show the electric field profile of the surface plasmon resonance mode at wavelength of 975 nm in the *xz* and *yz* planes, respectively. The electric field profile of the surface plasmon at this wavelength was similar to that at resonance wavelength of 643 nm with larger propagation length (decaying tail through the substrate and superstrate).

By changing the structure from the Au-SiO_2 to the Au-SiO_2-Au nanobelt structure, the electric field confinement was observed at the upper Au nanobelt and SiO_2 nanobelt interface with decaying tail in to the superstrate, as it is clear from Figs. 3g and 4d. The observation of decaying tail could be due to the phase velocity reduction effects due to the presence of SiO_2 nanobelt [14].

As can be seen from Fig. 4e, in addition to the surface plasmon resonance mode at wavelength of 975 nm, four symmetric (rectangular) hot zones were also recorded at the SiO_2/2nd Au nanobelt interface that could be attributed to presence of grating orders [17]. It can be concluded that coupling between the grating order resonance modes and surface plasmon resonance mode was led to strong confined hybrid surface plasmon mode at wavelength of 975 nm in the Au-SiO_2-Au nanobelt structure compared to the Au-SiO_2 nanobelt with electric field enhancement as high as 21× with respect to the incident electric field.

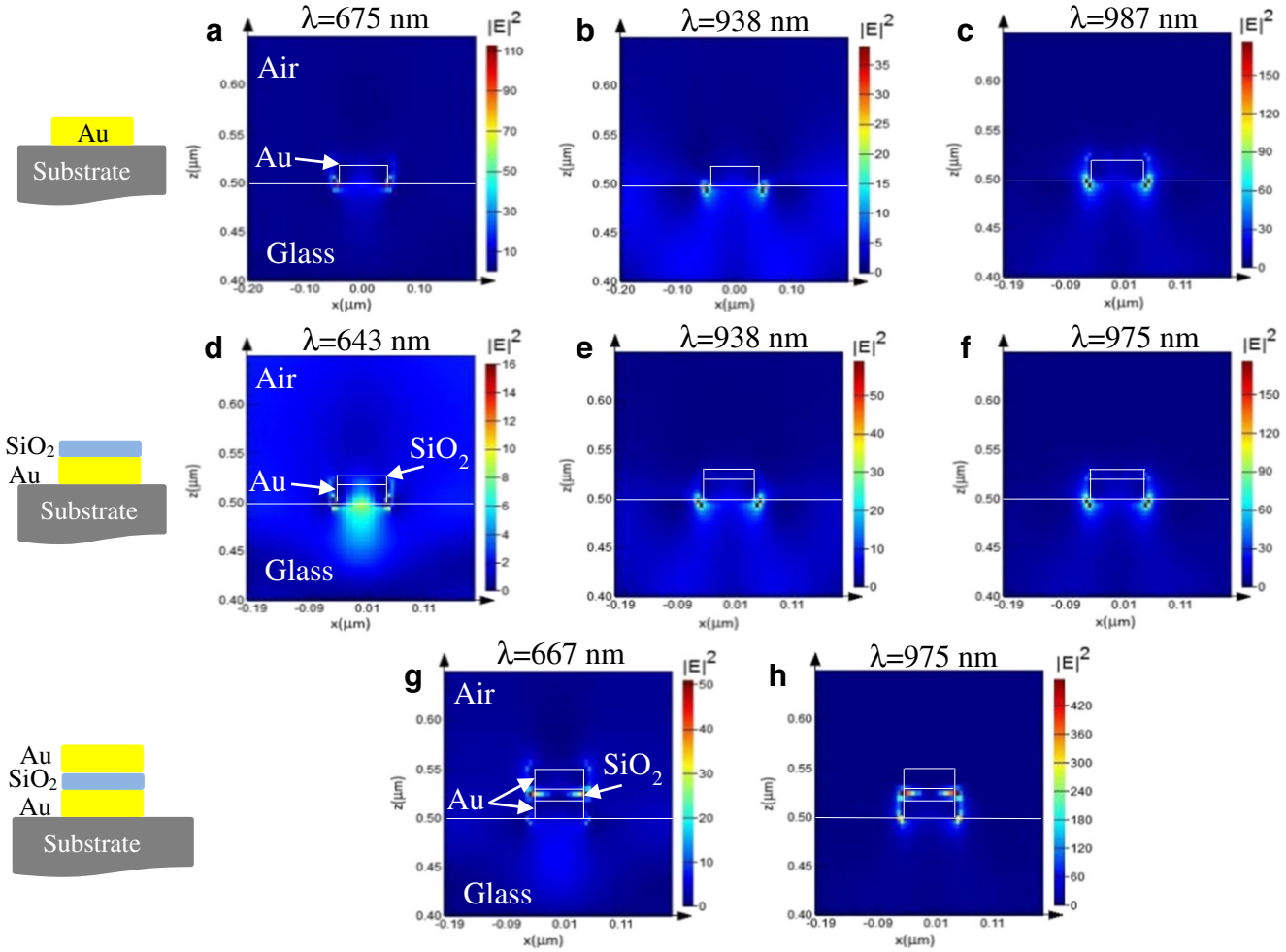

Fig. 3 *Top row*, the E^2 profile of single-layer Au nanobelt at resonance wavelength of **a** λ_{res}=675 nm, **b** λ_{res}=938 nm and **c** λ_{res}=978 nm. *Middle row*, the E^2 profile of the Au-SiO_2 nanobelt at resonance wavelength of **d** λ_{res}=643 nm, **e** λ_{res}=938 nm and **f** λ_{res}=975 nm. *Bottom row*, the E^2profile of the Au-SiO_2-Au nanobelt at resonance wavelength of **g** λ_{res}=667 nm and **h** λ_{res}=975 nm. The incident electric field was fixed at 1 V/m

The Effects of Varying Polarization Angle and Incident Angle of Light Source

The effects of varying polarization angle (α) of the incident EM field (plane wave source) on the extinction spectrum of the Au-SiO_2-Au structure were studied by varying the polarization angle of incident EM field from 0° (TM-mode) to 90° (TE-mode) by increment of 10°. Figure 5a shows extinction spectrum of the Au-SiO_2-Au nanobelt structure with 10 nm thick SiO_2 which was placed between the two Au nanobelts of height and width of 20 and 100 nm, respectively. As it is clear from this figure, by increasing the polarization angle the extinction resonance, peak intensity and its width were increased. It was also found that the resonance wavelength of LSPR mode was shifted towards smaller wavelengths by 15 nm; however, the resonance wavelength position of SPR mode was shown a red shift of 23 nm on increasing the polarization angle from 0° (TM-mode) to 90° (TE-mode) as it is evident in Fig. 5a. At polarization angles of 80° and 90° (TE-mode), there was not any SPR mode in the recorded extinction spectrum, whereas one extinction peak was recorded at wavelength of 991 nm as it is evident in Fig. 5a. The change in the extinction spectrum can be explained by the physics of the surface plasmon excitation. It is known that surface plasmon resonance is excited only when the momentum conservation is fulfilled between the incident EM wave at TM-mode and oscillating electron of the metallic surface.

Table 1 The resonance wavelength position and linewidth of different nanobelt structures

Nanobelt structure	Resonance position (nm)		Linewidth (nm)	
	PSPR	LSPR	PSPR	LSPR
Au	675	987	30	296
Au-SiO_2	643	975	-	296
Au-SiO_2-Au	667	975	175	128

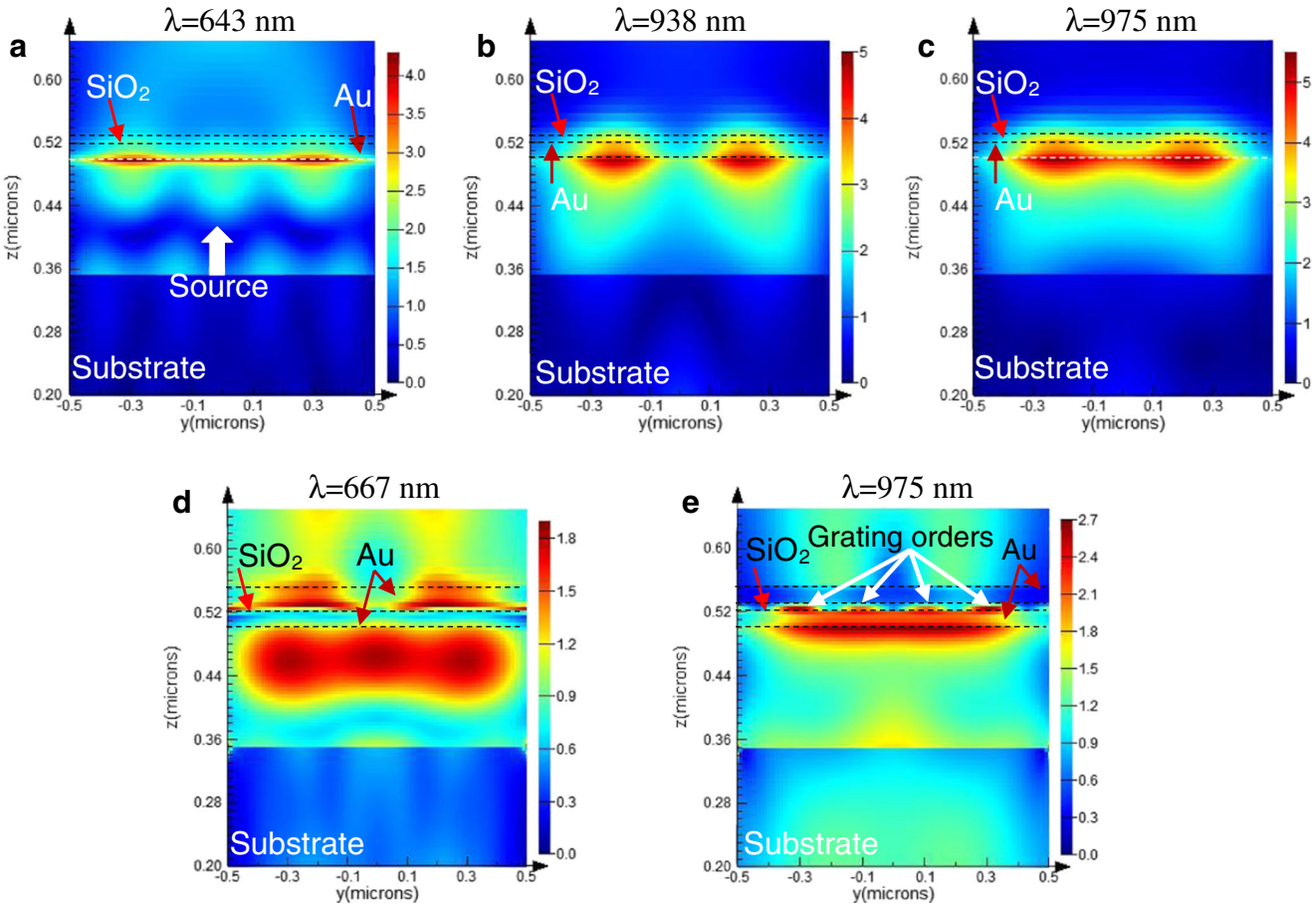

Fig. 4 Surface plasmon resonance profile along *y*-axis of the Au-SiO_2 (**a**–**c**) and the Au-SiO_2-Au nanobelt structures (**d**, **e**) with quasiperiod of 300 nm, nanobelt width and height of 100 and 20 nm, respectively, and 10 nm thick SiO_2

Hence, by changing the polarization angle from 0° (TM-mode) to 90° (TE-mode), momentum mismatch was raised between incident light wavevector, k_z, and surface plasmon polariton wavevector, k_{spp}, [3], which led to grating order resonance peaks instead of hybrid resonance mode and absence of the SPR mode at two polarization angles of 80° and 90°.

The effects of varying the incident angle (θ) of the plane wave at TM-mode (α=0°) in the range of 0° to 30° on the extinction spectrum of the Au-SiO_2-Au nanobelt structure

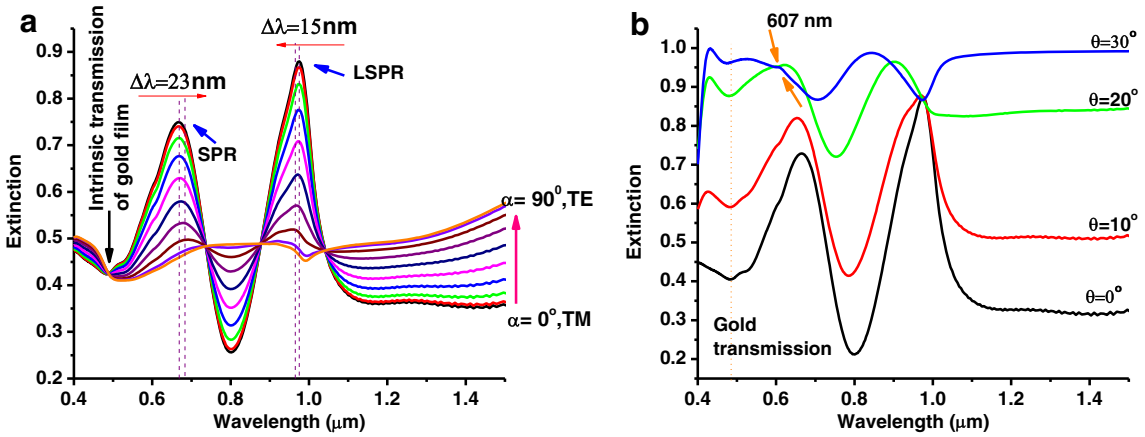

Fig. 5 The effects of varying the **a** polarization angle (α) and **b** incident angle (θ) on the extinction spectrum of the Au-SiO_2-Au-nanobelt structure with 10 nm thick SiO_2, Au height and width of 20 and 100 nm, respectively, structural period of 300 nm and ambient medium refractive index of 1.000. The incident angle (θ) and the polarization angle (α) of the incident plane wave was 0° in **a** and **b**, respectively

were compared in Fig. 5b. The extinction valley at 478 nm which is independent of incident angle (Fig. 5b) and polarization angle (Fig. 5a) was assigned to the intrinsic transmission of gold film which was discussed elsewhere [18].

As can be seen from Fig. 5b, the surface plasmon resonance intensity (extinction intensity) was reduced by increasing the incident angle. It is also clear that the resonance linewidth was increased, and the resonance wavelength position offers a blue shift especially for LSPR mode as a result of increasing the incident angle. More interesting effects were observed by using the EM field at incident angle larger than 20°. As it is clear from Fig. 5b, the extinction spectrum of the Au-SiO_2-Au nanobelt structure at incident angle of θ=30° depicts two extinction peaks at wavelengths of 607 and 843 nm. The former sharp peak (marked with orange arrows) could be attributed to the Rayleigh Anomaly [17], while the second one is the hybrid LSPR mode that was blue shifted by 132 nm compared to the extinction spectrum at incident angle of 0°. From Fig. 5b, it can be concluded that the transmission intensity of the Au-SiO_2-Au nanobelt at θ=30° was dropped to 0 beyond the wavelength of 1000 nm, whereas the recorded transmission was larger than 15 % beyond the LSPR mode at θ smaller than 30°.

Quasiperiodic Structure Variation

A series of numerical simulations were carried out to study the effects of varying the structural periodicity along *x*-axis on extinction spectrum of the Au-SiO_2-Au nanobelt structure. In these studies, the Au nanobelt height and width were fixed at 20 and 100 nm, respectively, and the SiO_2 height was fixed as 10 nm. The nanobelt length was chosen as 1 μm to avoid any Fabry-Perot resonance effects [4, 19]. The effects of varying the quasiperiodic structure along *x*-axis on the extinction spectrum at the air/Au interface of the Au-SiO_2-Au structure are shown in Fig. 6a for both PSPR and LSPR modes.

As can be seen from this figure, the linewidth of the localized surface plasmon mode was increased by increasing the structural periodicity along *x*-axis. Therefore, it can be concluded that smaller structural periodicity offers narrower linewidth compared to the larger one. It was also found that by increasing the structural periodicity along *x*-axis, the resonance wavelength of LSPR mode has a blue shift of 51 nm and the extinction intensity was reduced by ~35 % as it is shown in Fig. 6b. The reduction in the resonance extinction intensity could be attributed to weaker coupling effects of LSPR mode of the Au-SiO_2-Au structure with its closest neighbours. The LSPR mode coupling between two successive nanobelt structures was reduced by increasing their separation distance as the electric field amplitude of the surface plasmon mode was decaying exponentially [3].

Dielectric Height Variation

The effects of varying the spacer height on extinction spectrum of the Au-SiO_2-Au structure of 20 nm thick and 100 nm wide were studied numerically by varying the SiO_2 height in the range of 10 to 100 nm. In each numerical analysis, the extinction data was recorded at 250 nm away from the 2nd Au nanobelt (air/Au nanobelt interface). Fig. 7a shows the recorded extinction spectrum of the nanobelt structure at different spacer heights. It was found that by increasing the spacer height from 10 to 100 nm, the LSPR wavelength was shifted towards smaller wavelength and resonance wavelength was recorded at wavelength of 935 nm at dielectric height of 100 nm as it is also evident in Fig. 7b.

From Fig. 7b, it can also be seen that by increasing the spacer height from 10 to 40 nm, the linewidth of the LSPR mode was increased by 84 nm (green triangles), while by further increasing of the spacer height up to 100 nm, the

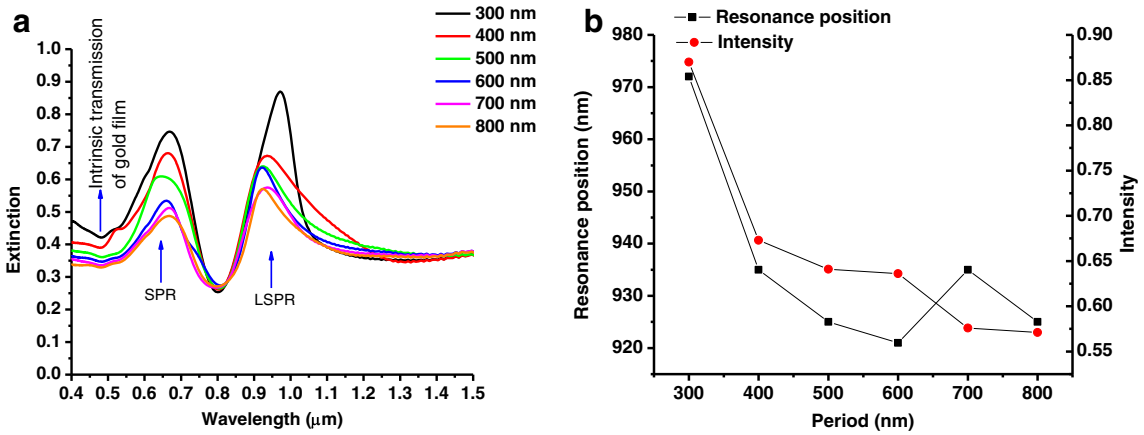

Fig. 6 The effects of varying the quasiperiodic structure along *x*-axis on **a** the extinction spectrum of PSPR and LSPR modes and **b** resonance position and extinction resonance intensity of LSPR mode. The Au height and width were fixed as 20 and 100 nm, respectively. The SiO_2 height, structure length along *y*-axis and refractive index of the superstrate layer were fixed at 10 nm, 1 μm and 1.0000, respectively

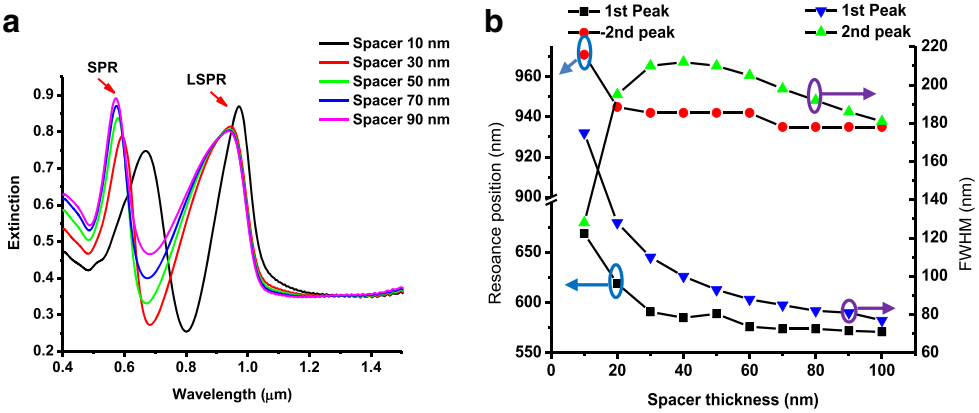

Fig. 7 The effects of varying the spacer height on the **a** extinction and **b** resonance wavelength and linewidth of both propagated and localized surface plasmon modes. The Au height and width were fixed at 20 and 100 nm for each nanobelt. The nanobelts length along *y*-axis was fixed at 1 μm. The superstrate layer was considered as air

linewidth of the LSPR mode was reduced by 29 nm. Furthermore, the linewidth of PSPR mode of the nanobelt structure was reduced monotically from 175 to 77 nm by increasing the spacer height from 10 to 100 nm (blue triangles). The minimum linewidth values for PSPR and LSPR modes were calculated as 77 and 181 nm, respectively, at dielectric height of 100 nm. The main reason for achieving narrower linewidth for PSPR modes could be attributed to more electric field confinement at larger spacer height, larger aspect ratio of the structure and smaller phase velocity of the surface plasmon resonance waves [4, 14] which increases the SPR absorption by medium and reduce its propagation length.

Surface Sensing

The effects of using liquids with different refractive indices in the range of 1.333 to 1.377 on the sensing properties of single-layer Au nanobelt structure and the Au-SiO_2-Au nanobelt structure with Au height and width of 20 and 100 nm, respectively, spacer height of 10 nm, nanobelt length of 1 μm along *y*-axis and quasiperiodic of 300 nm along *x*-axis were studied numerically. The surface of the nanobelt structure was covered by 250 nm thick liquids with refractive indices of 1.333, 1.345, 1.356, 1.367 and 1.377. Figure 8a, b shows the FDTD calculated extinction spectrum of the designed structures at different refractive indices of the superstrate medium.

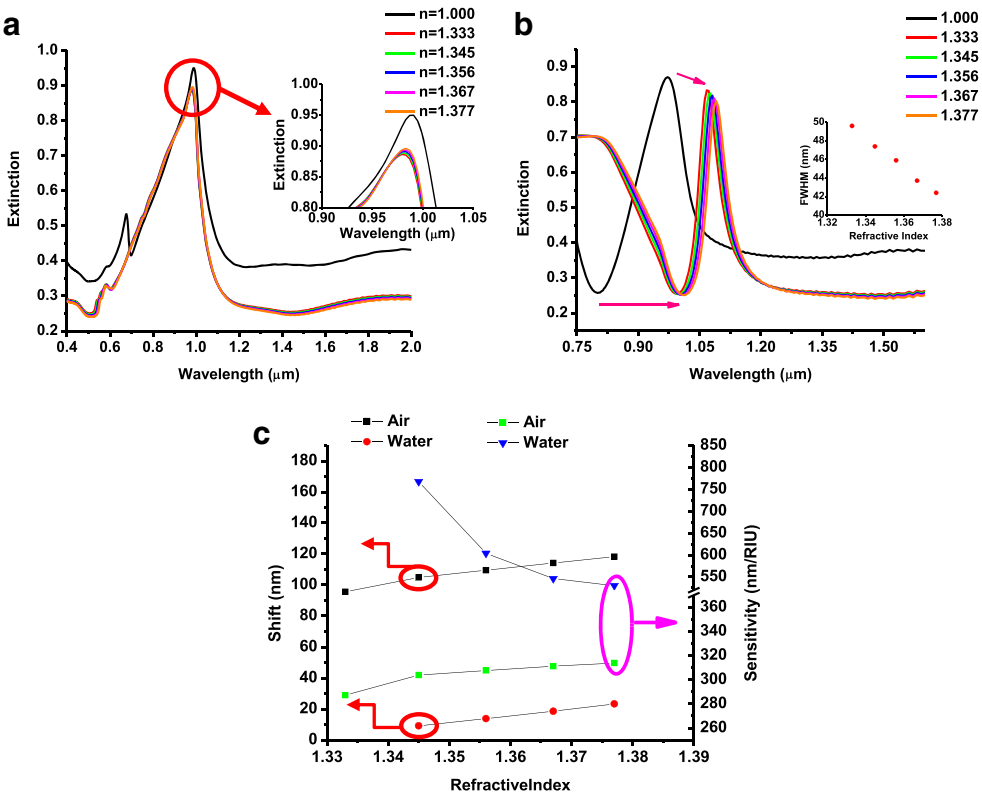

Fig. 8 FDTD calculated extinction spectrum of liquids with different refractive index as a function of wavelength for **a** single-layer Au nanobelt and **b** the Au-SiO_2-Au nanobelt structure. **c** Resonance wavelength shift and sensitivity of the Au-SiO_2-Au nanobelt structure as a function of refractive index for two different reference points of water and air. The height and width of both Au nanobelts and the SiO_2 height were fixed as 20, 100 and 10 nm, respectively. The nanobelt lengths along *y*-axis and quasiperiodic structure along *x*-axis were fixed at 1 μm and 300 nm, respectively

As it is shown in Fig. 8a, there was not any significant shift in the resonance extinction position at wavelength of 987 nm by increasing the liquid refractive index from 1.333 to 1.377; however, increasing the refractive index from 1.000 to 1.333 resulted in a 5 nm blue shift. It is also clear that by increasing the refractive index of the superstrate beyond 1.000, the resonance mode at wavelength of 675 nm disappeared which was also reported in Fig. 2d and discussed in "Extinction Resonance Spectrum (Normal Incidence, TM-Mode)".

The wavelength of hybrid surface plasmon resonance mode was shown with a red shift by increasing the refractive index of the surrounding medium as it is shown in Fig. 8b. It is clear that on using liquids with refractive index in the range of 1.333 to 1.377, the resonance wavelength was shifted almost linearly as it is also evident in Fig. 8c. It is well known that the resonance wavelength position strongly depends on the effective dielectric constant of the designated structure [20, 21], and the FWHM of the resonance wavelength was decreased by increasing the refractive index of the ambient medium [22, 23]. Therefore, observing the red shift in the resonance wavelength of the Au-SiO_2-Au nanobelt structure can be attributed to the increasing of the ambient refractive index and hence increases the effective dielectric constant of the structure.

From Fig. 8b, c, it can be concluded that the maximum resonance shift was acquired, by using a liquid with larger refractive index for both air and water reference points.

Figure 8c also depicts the resonance bulk sensitivity, which is equal to the ratio of resonance wavelength shift and refractive index change ($\Delta\lambda/\Delta n$), of the Au-SiO_2-Au nanobelt structure which they were calculated with respect to the air and water. It was found that larger sensitivity was calculated when it was measured with respect to the water ($n=1.333$) compared to that measured with respect to the air ($n=1.00000$). By using water as reference point, the maximum sensitivity of 768 nm/RIU was measured at refractive index change of 0.012 as it is clear from Fig. 8c, whereas by using air as the reference point, the maximum sensitivity of 313 nm/RIU was measured at refractive index change of 0.377.

It was also found that by increasing the refractive index, the linewidth of the LSPR mode was reduced linearly as it is clear from Fig. 8b inset. The minimum linewidth of 42 nm was calculated at refractive index of 1.377 while it was calculated as high as 128 nm at refractive index of 1.000. By comparing the linewidth of the hybrid SPR mode of both single-layer Au and the Au-SiO_2-Au nanobelt structures and their sensitivity properties, it can be concluded that the Au-SiO_2-Au nanobelt structure could be considered as a candidate for sensing chemicals with refractive index close to the water; however, this structure still cannot compete with the nanohole array structure [24, 25].

Conclusion

Optical properties of the nanobelt structures with quasiperiod along x-axis with optimum heights and widths of the nanobelts for both Au layers and dielectric spacer were investigated. It was shown that by increasing the dielectric layer height, the extinction spectrum was shifted towards smaller wavelength in the Au-SiO_2-Au nanobelt structure. It was found that the localized surface plasmon mode was shifted by 36 nm while the propagated surface plasmon mode was offered a blue shift by 98 nm.

The bulk sensitivity of both single-layer Au nanobelt grating structure and the Au-SiO_2-Au structure was compared by using air and water as reference points. It was found that by using water ($n=1.333$) as reference point, the sensitivity of the Au-SiO_2-Au nanobelt structure was at least 2.1 times larger than by using air ($n=1.000$) as reference point. The maximum and minimum bulk sensitivity was recorded as 768 nm/RIU and 287 nm/RIU for refractive index change of 0.012 and 0.333, respectively. It was also shown that the linewidth of the resonance wavelength was reduced by increasing the refractive index.

References

1. Atwater HA, Polman A (2010) Plasmonics for improved photovoltaic devices. Nat Mater 9(3):205–213
2. Lal S, Link S, Halas NJ (2007) Nano-optics from sensing to waveguiding. Nat Photonics 1(11):641–648
3. Maier SA (2007) Plasmonics:fundamentals and applications. Springer
4. Anderson LJE et al (2011) A tunable plasmon resonance in gold nanobelts. Nano Lett 11(11):5034–5037
5. Hutter E, Fendler JH (2004) Exploitation of localized surface plasmon resonance. Adv Mater 16(19):1685–1706
6. Homola J, Yee SS, Gauglitz G (1999) Surface plasmon resonance sensors: review. Sensors Actuators B Chem 54(1–2):3–15
7. Mayer KM, Hafner JH (2011) Localized surface plasmon resonance sensors. Chem Rev 111(6):3828–3857
8. Saber MG, Sagor R (2013) Characteristics of symmetric surface plasmon polariton mode in glass–metal–glass waveguide. Plasmonics 8(4):1621–1625
9. Zhu J, Huang X, Mei X (2012) A laser structure based on metal-dielectric-metal plasmonic nanocavity. Plasmonics 7(1):93–98
10. Liao H, Nehl CL, Hafner JH (2006) Biomedical applications of plasmon resonant metal nanoparticles. Nanomedicine 1(2):201–208
11. Sullivan DM (2000) Electromagnetic simulation using the FDTD method. IEEE Press Series, New York
12. Alexandre V, Thierry L (2007) Description of dispersion properties of metals by means of the critical points model and application to the study of resonant structures using the FDTD method. J Phys D Appl Phys 40(22):7152
13. Rakic AD et al (1998) Optical properties of metallic films for vertical-cavity optoelectronic devices. Appl Opt 37(22):5271–5283
14. Hohenau A et al (2005) Dielectric optical elements for surface plasmons. Opt Lett 30(8):893–895

15. Svelto O (2010) Principles of Lasers 5ed
16. Jackson JD(1962) Classical electro dynamics.Wiley
17. Hohenau A, Leitner A, Aussenegg F (2007) Near-field and far-field properties of nanoparticle arrays. In: Brongersma M, Kik P (eds) Surface plasmon nanophotonics. Springer, Netherlands, pp 11–25
18. Irannejad M, Yavuz M, Cui B (2013) Finite difference time domain study of light transmission through multihole nanostructures in metallic film. Photon Res 1(4):154–159
19. Belotelov VI et al (2012) Fabry-Perot plasmonic structures for nanophotonics. J Opt Soc Am B 29(3):294–299
20. Ebbesen TW et al (1998) Extraordinary optical transmission through sub-wavelength hole arrays. Nature 391(6668):667–669
21. Carretero-Palacios S et al (2012) Effect of film thickness and dielectric environment on optical transmission through subwavelength holes. Phys Rev B 85(3):035417
22. Dostálek J, Kasry A, Knoll W (2007) Long range surface plasmons for observation of biomolecular binding events at metallic surfaces. Plasmonics 2(3):97–106
23. Lee K-S et al (2010) Resolution enhancement in surface plasmon resonance sensor based on waveguide coupled mode by combining a bimetallic approach. Sensors 10(12):11390–11399
24. Brolo AG et al (2004) Surface plasmon sensor based on the enhanced light transmission through arrays of nanoholes in gold films. Langmuir 20(12):4813–4815
25. Irannejad M, Cui B, Yavuz M (2015) The effects of varying dielectric spacer height on the reflection resonance spectrum of gold nanorod-on-mirror grating structure. Plasmonics. doi:10.1007/s11468-015-9878-5